Doc Ophthalmol (2013) 126:125–136
DOI 10.1007/s10633-012-9366-6

ORIGINAL RESEARCH ARTICLE

Dichoptic multifocal visual evoked potentials identify local retinal dysfunction in age-related macular degeneration

Faran Sabeti · Andrew C. James · Rohan W. Essex · Ted Maddess

Received: 10 July 2012 / Accepted: 3 December 2012 / Published online: 13 December 2012

Abstract
Purpose To evaluate the ability of multifocal visual evoked potentials (mfVEPs) to identify functional loss in patients with early and exudative age-related macular degeneration (AMD). A dichoptic multifocal stimulus presentation was employed to investigate the regional effects of AMD and the potential diagnostic utility in macular disease.
Methods MfVEP responses were recorded from 19 unilateral exudative AMD patients with non-exudative ($n = 15$) or normal ($n = 4$) presentations in the fellow eye and 28 age-matched controls. Root mean square (RMS) waveforms were pooled across selected EEG channels to produce global field RMS (gfRMS) waveforms. GfRMS amplitudes and response delays were analysed by multivariate linear models, and diagnostic capacity was measured using areas under the curve (AUC) of receiver operator characteristic plots.
Results The mean gfRMS amplitude of the exudative eye of AMD patients was significantly reduced compared with the controls (-2.03 ± 0.08 dB, $t = -12.9$). Fellow non-exudative AMD eyes were less effected but still significantly reduced (-0.84 ± 0.07 dB, $t = -11.5$). No significant difference in mean gfRMS delay of AMD eyes across the central 46° was observed. AUC values of 100 ± 0.0 % (mean ± SE) for exudative and 79.7 ± 6.5 % for non-exudative eyes were obtained for response amplitudes.
Conclusion The study demonstrated that mfVEP identified retinal dysfunction in both exudative AMD and fellow non-exudative AMD eyes, but mostly affecting the macular field. The reduced testing duration and good diagnostic accuracy suggest that dichoptic mfVEPs may be a sensitive tool for monitoring progression in AMD.

Keywords Multifocal · Visual evoked potentials · Age-related macular degeneration

F. Sabeti (✉) · A. C. James · R. W. Essex · T. Maddess
ARC Centre of Excellence in Vision Science, John Curtin School of Medical Research, The Australian National University (ANU), Canberra, ACT 0200, Australia
e-mail: faran.sabeti@anu.edu.au

R. W. Essex
Ophthalmology Department, Canberra Hospital, The Australian National University, Canberra, ACT, Australia

Introduction

Conventional visual evoked potentials (VEPs) have been used for evaluation of optic neuropathies for many years [1–3]. Recently, multifocal VEPs [4] (mfVEPs) have allowed for high spatial resolution of stimuli to be used providing a rapid method for measuring responses from a large number of retinal locations. This technique improved diagnostic utility in optic nerve [5, 6] and retinal disease [7, 8].

It is well established that individuals with macular disease have reduced VEP amplitudes and delayed latencies [9–15]. However, disagreements have emerged over the latencies observed between retinal and optic nerve disease [7, 13–15]. The clinical implication is that abnormal cortical responses from optic neuritis may be indistinguishable from retinopathy and indeed has been postulated by some authors [7, 13]. Furthermore, some investigators have reported a strong correlation between visual acuity, central visual field sensitivity and latency [16], while others have reported VEP delays in maculopathy patients with normal or near-normal visual acuity [9, 12] and poor correlation with scotoma size [14]. Other than preliminary reports from our laboratory, and one case study, there have been no reports of mfVEP responses in AMD [7, 17]. Previous studies have used conventional pattern VEPs for evaluation of macular disease and so are limited by relatively low spatial resolution. Hence, our knowledge of the effects of macular disease on cortical response properties from multiple visual field locations remains effectively unknown.

The purpose of this study was to examine the effects of age-related macular degeneration (AMD) on mfVEP responses using an 84-region/eye dichoptic stimulus presentation method. To compare the relationship between early- and end-stage disease, we examined patients with exudative AMD and contralateral early AMD presentations. We employed a new variant of mfVEP stimuli which were temporally sparse [18–20] and have been shown to have high diagnostic accuracy in multiple sclerosis [5]. Enhancement in stimulus parameters may help distinguish macular disease and improve diagnosticity in preclinical presentations. Accordingly, the diagnostic utility of the new method was assessed.

Methods

Subjects

Twenty-three individuals with unilateral choroidal neovascularization (CNV) secondary to AMD were recruited from the ophthalmology clinic at The Canberra Hospital. Four patients were excluded from the study due to noisy recordings. Subjects were diagnosed following best-corrected visual acuity (BCVA), fundus biomicroscopy, fluorescein angiography and OCT (Zeiss Cirrus: Carl Zeiss Meditec Inc. Dublin, California, USA) and were concurrently being treated with ranibizumab (Lucentis, Novartis, North Ryde, NSW) injections in the affected eye. The mean age was 77.7 ± 5.4 years (11 females), range 61–85. The mean corrected logMAR visual acuity was 0.75 ± 0.56 (mean $\pm$ SD) for exudative AMD eyes. The fellow eye had a normal ($n = 4$) or non-exudative AMD ($n = 15$) fundus appearance defined by the presence of drusen and/or retinal pigmented epithelial (RPE) changes with a BCVA of 0.3 or better. Subjects were excluded if they had any previous or current ocular or neurologic disease, constant tropia or were on medication known to affect retinal function.

Twenty-eight control subjects had an age range of 59–88 years, mean 70.78 ± 6.11 (18 females). The inclusion criteria were BCVA of 0.0 or better, normal intraocular pressure, fundoscopy and Frequency Doubling Perimetry C-20 fields and no family history of AMD.

All subjects were informed of any potential risks prior to participation and gave informed written consent. This research was approved by ANU Human Research Ethics Committee and adhered to the tenets of the Declaration of Helsinki.

Stimulus and recording

The stimulus consisted of an 84-region cortically scaled [4] dartboard layout (Fig. 1) subtending a total diameter of 46°. The eccentricities of the region centres were 1.6°, 3.0°, 4.8°, 7.1°, 10.2°, 14.3° and 19.8° comprising seven concentric rings, each containing 12 test regions. A small fixation cross occupied the central 1°. All recordings were performed binocularly, and stimuli were presented dichoptically at a 60 Hz refresh rate. Trial lenses compensated for refractive errors to within 1.5 dioptres of the subject's ametropia. Independent stimuli were directed to each eye concurrently by displaying them on separate LCD monitors through a stereoscopic system (Truefield Analyzer; Seeing Machines Ltd., Acton, ACT Australia) [18, 19]. The temporal stimulus delivered to each region was based on a sparse pattern pulse presentation, which has been detailed elsewhere [18]. The pseudorandom sequence was optimized for maximal spatial sparseness to minimize interactions between active neighbouring stimuli [21]. Each region contained 16 checks—eight white (180 cd/m^2) and eight black (1 cd/m^2)—and was pulsed on for 33 ms. When no checkerboard was present, the monitor was maintained at 90 cd/m^2. Recording run duration was 240 s divided into eight segments of 30 s, and subjects were allowed to rest between segments if they wished. Subjects completed the test twice on the same day to assess repeatability.

Electrical signals were recorded from 64 channels using pin-type active Ag–AgCl electrodes (Actiview, Biosemi Ltd., Amsterdam). The ground electrode was placed on the right earlobe. Signals were amplified 50,000 times and filtered with a bandpass of 1–20 Hz. These data were simultaneously sampled and collected by data acquisition software (Active2, BioSemi software, Biosemi Ltd., Amsterdam). A correctly sized head cap with 64 electrodes in a 10–10 layout was placed over the subjects' head reference to the inion. Electrode holders on the head cap were filled with gel (Spectra 360 Gel, Parker Laboratories Inc., Fairfield, New Jersey), and electrodes were pushed into the holders. Representative responses are shown in Fig. 2.

Data analysis

The recordings were transferred to MATLAB® for data analysis (R2009b, The MathWorks, Natick, MA). The method for estimating the mean response to stimuli presented at each region has been described in detail elsewhere [18, 19]. The following is a brief summary of the methods employed in this study. It was desirable to combine responses from different electrodes, and sometimes different visual field regions, subjects and so on. VEP response waveforms from different parts of the visual field can have different shapes and are commonly inverted for visual field locations in the superior and inferior visual fields (e.g. Fig. 2a, b). Perhaps more importantly, since there were 84 stimulus regions/eye and 64 electrodes, there were $64 \times 2 \times 84 = 10{,}752$ responses recorded from each subject on each repeat. Therefore, in order to make use of this large amount of data, we pooled collections of waveforms from selected visual field locations and electrodes by computing computed root mean square (RMS) at each time point of each

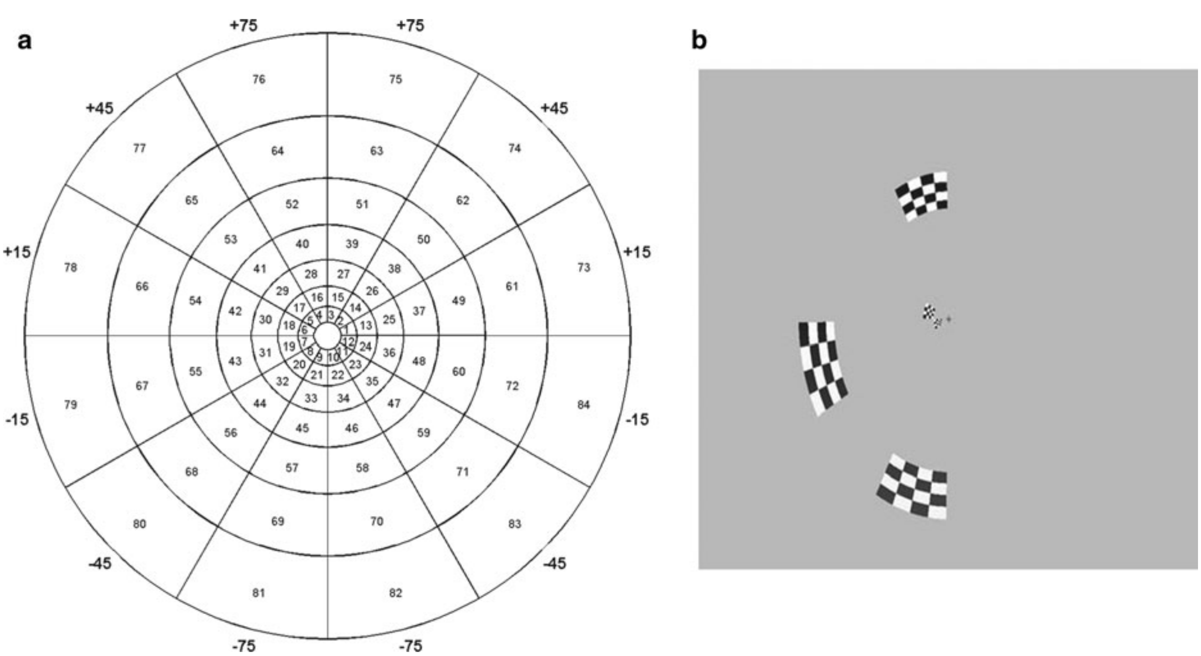

Fig. 1 **a** 84-region dartboard with corresponding region numbers. The dartboard is scaled according to the human cortical magnification factor. **b** Illustrative example of dartboard stimuli as seen by participant with the binocular displays verged. The sparsely presented stimuli meant that on a given presentation a test region rarely had a neighbouring region that was also active. The innermost edges of each ring were at 1.0°, 2.3°, 3.8°, 5.9°, 8.6°, 12.2° and 17.0°, and the outer edges were at 2.2°, 3.7°, 5.7°, 8.3°, 11.8°, 16.4° and 22.6° eccentricity

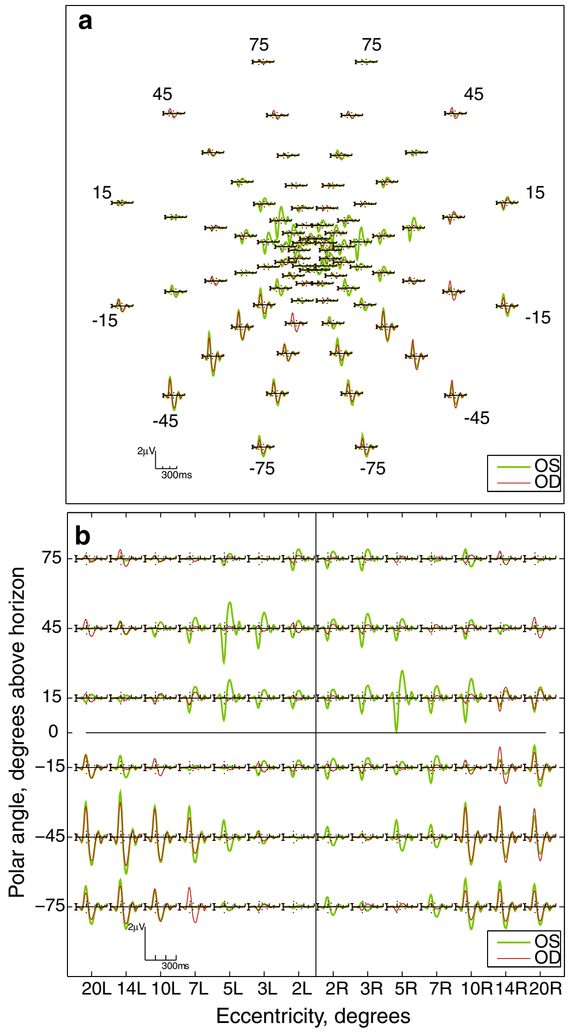

Fig. 2 **a** Example of multifocal VEP waveforms recorded from electrode POz for the AMD subject 620. Responses from OD (exudative AMD) and OS (non-exudative AMD) have been superimposed. **b** Rectilinear polar plot of VEP waveforms in (**a**) for subject 620, channel POz. The *x* axis represents the eccentricity (*left* and *right* visual fields), and the *y* axis represents the polar angle deviation upwards from the horizon. The representation is thus related to the map on the *left* and *right* hemi-cortices of V1. It also provides a clearer view of all the waveforms (cf. **a**)

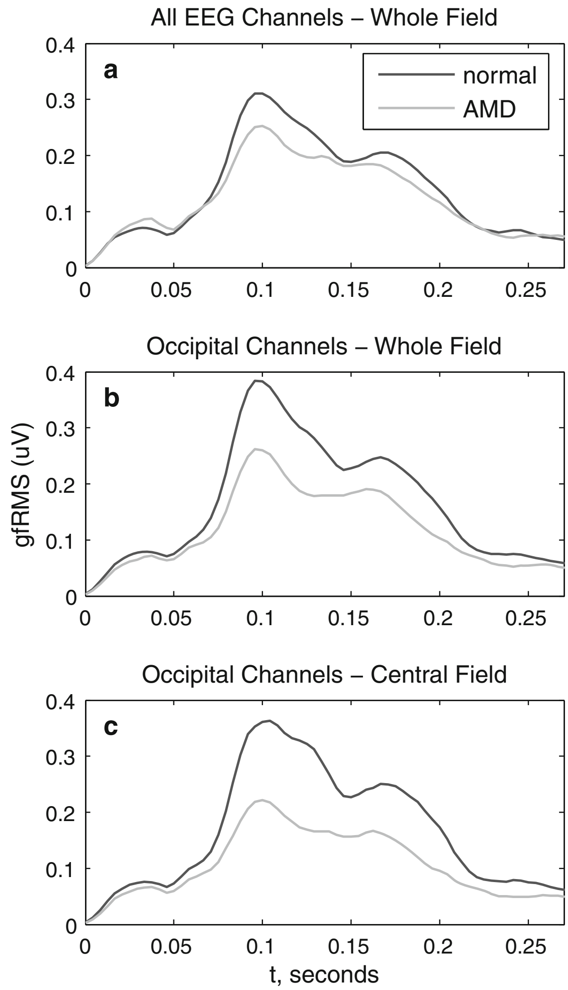

Fig. 3 Comparison of pooling response waveforms across different collections of EEG electrodes and visual field locations using the global field RMS (gfRMS) method. **a** gfRMS waveforms for normal and AMD subjects pooling across all 64 electrodes and visual field locations. **b**) gfRMS waveforms from occipital electrodes ("Methods") and all field locations. **c** gfRMS from the central 24 regions of the field (7.4°), recorded from the occipital channels. In general, responses from AMD subjects were smaller than those obtained from normal subjects with responses recorded from macular regions most affected

waveform across the selected EEG channels to create a so-called *global field RMS* (gfRMS) waveform. To pool waveforms across other factors such as subject and visual field locations, the median at each time point of the collection of gfRMS waveforms was then computed. The electrodes of interest in this study were either: all electrodes or eight occipital channels: POz, PO1, PO2, Oz, O1, O2, Iz and Pz. The effect of computing the gfRMS across different sets of electrodes and visual field locations is illustrated in Fig. 3. For most analyses, however, we did not average across stimulus regions or eyes so that there was one gfRMS waveform preserving the ability to detect regional loss as in any other mfVEP (Fig. 4).

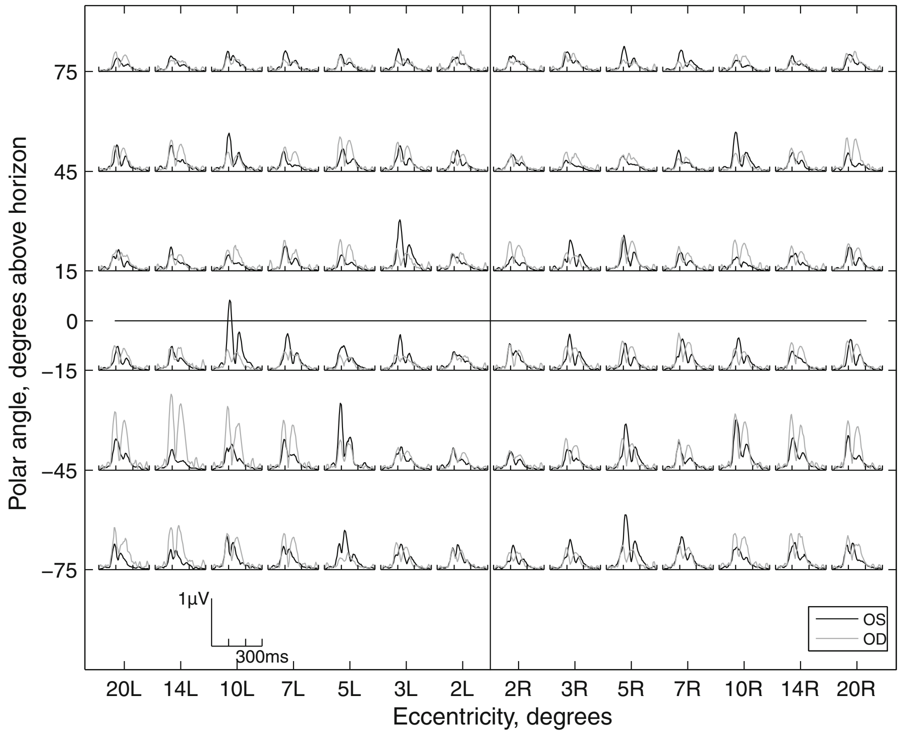

Fig. 4 Illustration of the gfRMS waveforms from occipital channel records from subject 620 VEP. Note the smaller variations in waveform shape and between-eye difference compared to the raw VEP waveforms (Fig. 3b) due to the pooling of responses across recording channels. It is evident that the gfRMS waveform shapes are similar at all locations to global waveforms (cf. Fig. 3), and in particular, the first peak is fairly stereotypical in its form (relative to the second peak); hence, amplitudes and delays of this feature were employed in later analyses

Multiple regression models were used to account for the independent effects of age, gender, visual field eccentricity and AMD on responses. Peak gfRMS responses were first log-transformed to decibels to balance the heteroskedastic variance. The effects of those independent factors were fitted as contrasts to a reference value. The reference variable represented the mean response of normal male subjects aged 75 years. To describe the agreement between repeated measurements, we used Bland–Altman analysis to determine the coefficient of repeatability (CR) and the mean difference [22]. Data are presented as mean ± standard deviation.

Receiver operator characteristic (ROC) plots were constructed to estimate the sensitivity and specificity for AMD using the regional deviations from the normative data. We utilized the area under the curve (AUC) of ROC plots to summarize the diagnostic performance of our method. Amplitude and delay asymmetry between eyes was included for exudative AMD, that is, the difference in between-eye (*asymmetric*) regional deviations relative to normal for both response parameters, a method that has previously shown utility in mfVEPs [6] and multifocal pupillography [23, 24]. For non-exudative AMD eyes we evaluated within-eye deviations of each region from the normative data.

Results

The gfRMS response strength averaged over all electrodes and visual field locations was 0.26 ± 0.03 µV ($p < 0.0001$) for the control group. The occipital channels alone gave larger gfRMS responses, with a mean of 0.39 ± 0.02 µV ($p < 0.0001$). Examples of response waveforms for each of the 84 stimulus regions recorded from channel POz are shown in Fig. 2. The response waveforms were obtained from an 85-year-old female with exudative AMD in the right eye and early AMD in the fellow eye. Best-corrected visual acuities were 0.8 in the right eye and 0.1 in the left eye. These responses identify reduced amplitudes in the central visual field of the right eye with delays in latency less evident.

We attempted to overcome the significant inter-subject variations in VEP responses due to the anatomy of the striate cortex among individuals [25, 26] by using a global metric, the *global field RMS* (gfRMS, "Methods"). Figure 3 shows the comparison of gfRMS waveforms computed across selected channels and regions in AMD and control groups. Compared to using all channels (Fig. 3a), larger differences in gfRMS strengths were achieved by selecting the occipital channels providing a peak amplitude of 0.38 ± 0.18 μV in the control group and 0.26 ± 0.12 μV in the AMD group (Fig. 3b). In a further refinement, determining the gfRMS from the central 2 stimulus rings (24 regions) achieved comparatively high amplitudes for controls (0.36 ± 0.17 μV, mean ± SE) but had the lower peak amplitude for AMD subjects (0.22 ± 0.09 μV) (Fig. 3c). Figure 4 illustrates the gfRMS waveforms computed across the occipital channels for the VEP responses of the same subject as in Fig. 2.

Table 1 summarizes the results of a multiple regression model examining the independent mean effects that various factors had on the per region gfRMS peak amplitudes and latencies. In the case of amplitudes the data were transformed to decibels ($10 \log_{10}$). Aside from stabilizing the variance, the decibel transformation allowed multiplicative effects to be fitted with an additive model. The top row of Table 1 gives the reference condition (the global mean for normal males aged 75 years). The remaining rows show the differences (*contrasts*) from the reference condition. Females had responses that were 1.61 ± 0.04 dB larger (1.4 times). The mean gfRMS amplitude for the reference condition was −4.81 ± 0.18 dB. Converting back to microvolt units gives a mean gfRMS amplitude of 0.33 μV. Subjects with exudative AMD had response amplitudes that were 0.63 times (−2.03 ± 0.08 dB) those of normal subjects. Responses from the central four (macular) rings, which extended to 8.3° eccentricity, were 39 % of those of normal subjects (−2.14 ± 0.10 dB). Eyes with non-exudative lesions had less mean amplitude deviation from normal overall (−0.84 ± 0.42 dB) and for the extra macular component (−1.10 ± 0.09 dB). To address the possibility that responses from one channel (cf. Fig. 2b) may produce larger effects than the gfRMS, we examined the mean effect of AMD on the amplitude responses measured only at channel POz. Mean effect sizes were 27 % smaller for exudative AMD (−1.48 ± 0.06 dB, $t = -24.3$) and 46 % less for non-exudative AMD (−0.45 ± 0.12 dB, $t = -3.7$) on POz amplitudes. We also investigated the independent effect of diagnosis on gfRMS time-to-peak response with a similar regression model. The reference time to peak was 102.2 ± 0.92 (ms ± SE). Aside from gender and age, the only significant effect was the modest reduction in macular delay for exudative AMD of −2.29 ± 0.53 ms. We also examined time to half-height and other earlier implicit times, and these made the reduction in time somewhat larger; hence, this was not an effect of fluctuations in the shape of the peak. The effect of age was also a small reduction in peak time of <1 ms/decade of age relative to the median of 75 years. Removing this effect of the model did not change the fitted values for the other factors.

Multiple regression showed that the effect of repeated measurements performed at the same visit did not reach significance (−0.03 ± 0.04 μV, $p < .5$) and the mean differences between repeats were 0.02 ± 0.25 μV and −0.003 ± 0.20 μV for normal and exudative AMD subject, respectively. The CRs for normal subjects were 0.39 and 0.49 μV for exudative AMD eyes.

Figure 5 shows the resulting mean region-by-region amplitude deviations from normal eyes for non-exudative AMD (Fig. 5a) and exudative AMD (Fig. 5b). We observed a bias towards greater amplitude loss in the superior hemifield in non-exudative AMD with sixty-four regions reaching significance ($p < .05$). In contrast, mean regional deviations in exudative AMD were biased towards the macula with 86 % of the overall field significantly smaller than normal.

In addition, mean regional delays also suggested central dysfunction in exudative AMD (Fig. 6b). Fifteen regions in the macular field (central four rings) were significant compared to only three regions within the outer three rings. Fourteen regions (83 %) across the field had significantly shorter time-to-peak responses than normal eyes. Delay effects for non-exudative AMD eyes followed a similar trend with nine out of 13 significant regions located in the macula. Ten regions (76 %) had significantly quicker time-to-peak responses.

Figure 7a illustrates the mean gfRMS amplitude for exudative and non-exudative AMD subjects plotted according to eccentricity (ring averages). These ring averages were computed via a linear model like that of Table 1 but where the mean values for each ring were estimated rather than just macular versus global effects. Recall from the methods that the independent effect of each ring was determined relative to a reference ring (mean response of ring 1 for male control subjects). Although ring analysis may be influenced by non-uniform pathology across the retina, there is histological evidence of significant photoreceptor loss in a ring-shaped pattern in the parafovea [27]. The mean gfRMS

Table 1 Summary of independent effects on gfRMS amplitude and latency for the various groups estimated by a multivariate linear model

Variable	gfRMS amplitude			gfRMS peak time		
	dB	SE	*t*	ms	SE	*t*
Reference	−4.81	0.18	27.2	102.2	0.92	111
Gender (female)	1.61	0.04	41.2	**2.89**	0.20	14.2
Non-exudative AMD	−0.84	0.07	11.5	0.11	0.39	0.28
Extra at macula	−1.10	0.09	3.95	−0.72	0.49	1.47
Exudative AMD	−2.03	0.08	12.9	0.73	0.43	1.72
Extra at macula	−2.14	0.10	11.6	**−2.29**	0.53	4.30
Decade of age relative to 75 years	−1.07	0.50	12.3	**−0.92**	0.17	5.33

Summary of two linear models quantifying effects on peak gfRMS amplitude and delay (rightmost three columns). The column's labelled variables indicate fitted factors. Since many of the effect sizes are quite large, the t-statics are reported rather than p-values. For the response amplitudes were all significant at $p < 10^{-4}$. The reference condition represents mean responses from male control ($n = 10$) subjects. With two exceptions the factors (and the covariate age, expressed as decades relative to the median of 75 years) quantify the difference from the reference. The exceptions are the extra changes observed within the macular area (the central four stimulus rings, $< 8.3°$ eccentricity) where the fitted values are the extra amount relative to the mean effect of either early or exudative AMD, and the t-values indicate the effect size relative to the mean effect of that disease. Amplitudes were transformed to decibels to allow for multiplicative effects to be fitted and to stabilize the variance. A positive effect for peak time indicates the additional delay produced by the variable. For peak times only the extra macular delay for exudative AMD, age and gender were significant (bold, $p < 10^{-4}$). Responses were smaller, especially in the macula. The only significant effect of AMD was a quickening of the time to peak centrally. Female responses were larger and slower, and all responses got slightly quicker with age

amplitude of exudative AMD eyes was significantly lower than non-exudative AMD in the central four rings (macula). The mean RMS time-to-peak responses across rings (Fig. 7b) illustrated the effects described in Table 1. Here, exudative AMD decreased mean time to peak within the central three rings (extending from 1.0° to 5.7° eccentricity, cf. Fig. 6), whereas non-exudative AMD eyes were less affected with significantly quicker time-to-peak responses in rings 1 and 3. Beyond the borders of the macula, time-to-peak responses for AMD were slower than for normal, although as Fig. 6 shows this is quite variable. We also examined region-wise effects and found no significant trends.

We next examined ROC curves to determine the diagnostic power of regional visual field deviations from normal fields. Amplitude and peak time between-eye *deviation scores* for exudative AMD (Fig. 8a) and within-eye deviations for non-exudative AMD (Fig. 8b) for the 20 worst (*N-worst*) visual field regions were considered. Amplitude deviations achieved the highest percentage area under the curve (AUC) of the ROC plot for both exudative (100 ± 0.0 %) and non-exudative (79.7 ± 6.5 %) AMD. Evaluating the mean percentage AUC obtained for the worst deviating regions of the visual field confirms the presence of a small number of severely dysfunctional regions in exudative AMD followed by a decline in AUC values for both amplitude and peak time variables. Measuring within-eye deviations in non-exudative AMD from mean normal data produced relatively poor AUC values. In addition, we evaluated the AUC values for the second peak of the gfRMS waveform (Fig. 3) and observed a reduction in diagnostic accuracy for exudative and non-exudative AMD (71.1 ± 8.8 % and 69.4 ± 8.6 %, respectively). Amplitude responses provided minimal improvement over peak time in eyes with milder macular pathology.

Discussion

The purpose of this study was to examine responses and diagnosticity in early and late stages of AMD using dichoptic stimulation of 84 regions using a sparse pattern pulse mfVEP. While conventional VEPs measure amplitude attenuation and delayed latencies in AMD [12, 15, 28, 29], it is not a distinguishing attribute because it is also found in eyes with other macular diseases [12, 15] and in optic neuropathy [11–14]. The use of higher-resolution mfVEP techniques may define local effects with

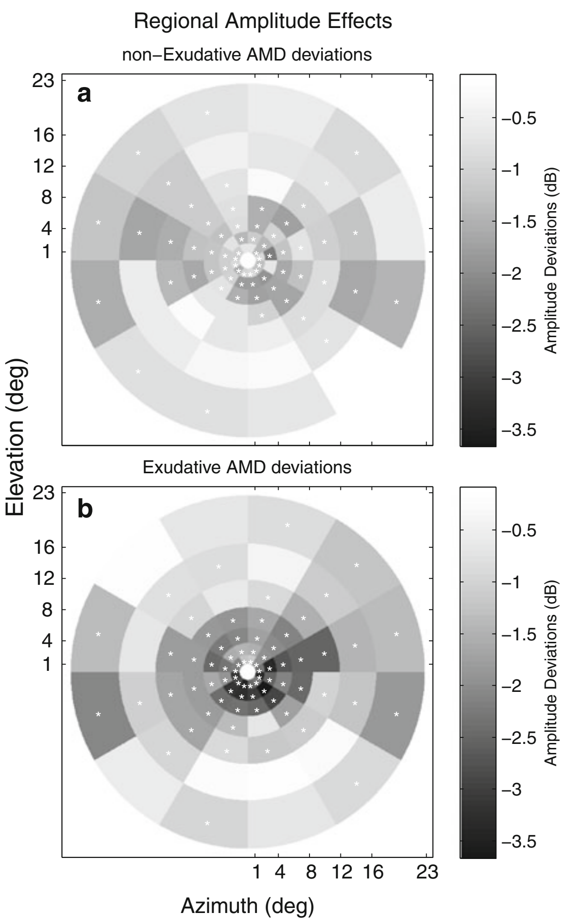

Fig. 5 Regional mean amplitude deviations for **a** non-exudative and **b** exudative AMD subjects. Regional responses for AMD subjects are expressed as mean deviations from normative data for each region. The mean amplitudes are across subjects, eyes and occipital channels and were transformed to dB to allow the fitting of a multiple regression model corrected for gender and age. The average regional deviations for non-exudative AMD (**a**) show a bias towards greater amplitude loss in the superior regions of the field. Sixty-four regions had a significant decrease in amplitude compared to normal (*$p < .05$). Regional deviations in (**b**) demonstrated a more typical profile for exudative AMD with the central field the site of greater sensitivity loss. Seventy-three of the darkest regions in (**b**) are statistically smaller than normal. Response amplitudes from left and right eyes have been combined by reversing the results of the right eye such that each region represents the identical segment of the field for each eye; thus, the temporal field is on the *left*. In both **a** and **b** the background (and *central*) grey level represents a deviation of 0 dB

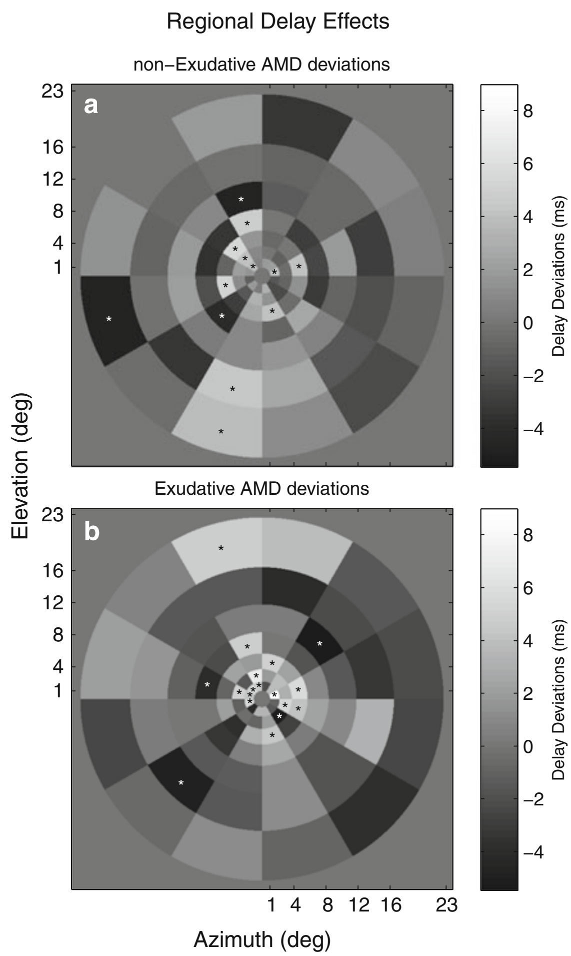

Fig. 6 Regional mean peak time deviations from normal. **a** The average response delays in non-exudative AMD subjects. The figure set-up is similar to Fig. 5 except that regions darker than the background represent longer delays. Ten regions across the field had significantly quicker time-to-peak responses than normal eyes with eight regions located in the macula (*$p < .05$). **b**) Delay effects for exudative AMD subjects were consistent with regions of reduced amplitudes in Fig. 5b. Shorter mean delays of fourteen regions in the field reached statistical significance with thirteen regions falling within the macular field. Only four regions predominantly in the outer rings had significantly longer time-to-peak responses. The *background grey level* represents a deviation of 0

greater accuracy and have potential clinical applications for diagnosis and monitoring of retinal disorders. In addition, comparing intraocular responses measured concurrently eliminates a source of variance improving diagnosticity in asymmetric disease presentations [6, 18, 30].

In this study exudative AMD had larger effects on mfVEP amplitudes than response delays. We observed a significant mean amplitude depression in the central four rings (eccentricity, 0°–8.3°) in exudative AMD eyes ($p < .005$) while the peripheral three rings (eccentricity,

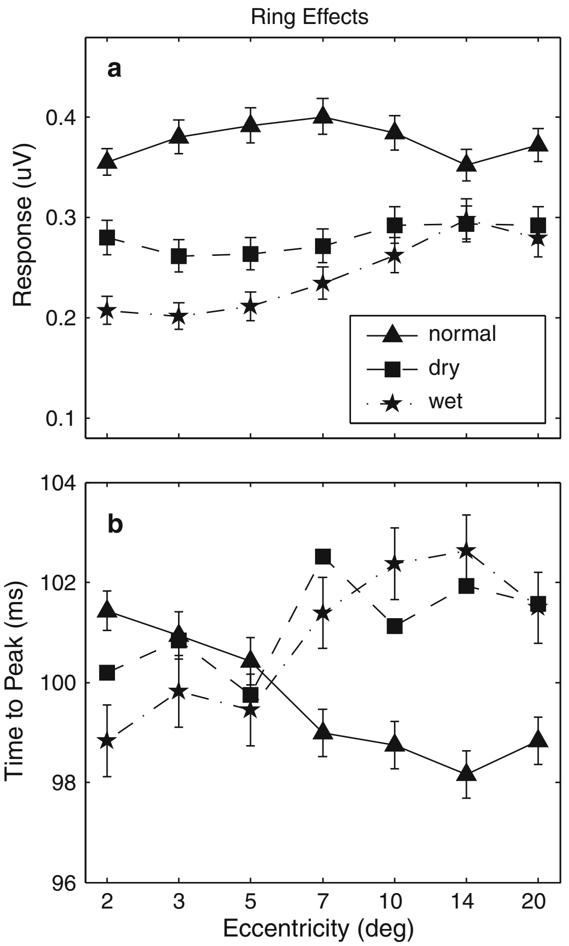

Fig. 7 The output of a linear model like that of Table 1 but where mean responses were computed for each ring of the stimulus array. Results are shown for normal, dry (non-exudative) and wet (exudative) AMD eyes. **a** gfRMS amplitudes show both global and central suppression of responses for patient eyes, with larger central changes in exudative AMD. *Error bars* are 95 % confidence limits. **b** Delay effects were less clear but showing the central delays and peripheral enhancement hinted at in Fig. 6. *Error bars* are standard errors

8.7°–22.6°) were only marginally significant (Table 1). Reduced amplitudes were found in eyes with early macular disease despite their good acuity. Our results are in agreement with the findings of Bass et al. [12] that about 50 % of contrast reversal VEP responses were delayed, in the sense that responses to a large single stimulus might be expected to mimic the peripheral delays seen here. MfERG responses have been reported to be abnormal in early AMD eyes with near-normal vision [31]. The innermost ring of those retinally scaled stimuli summed responses from 1° to 4° and so may have obscured the parafoveal effects reported here for M-scaled stimuli. On average, mfVEP abnormalities observed here in early AMD were not spatially associated with reported histological evidence of initial rod loss in the parafovea [27]; rather, amplitude loss peaked at ring 4 (mean eccentricity, 7.1°, cf. Fig. 7a) just beyond the borders of the parafovea. The implication is that mfVEP deficits may occur beyond regions of clinically visible pathology and suggests that non-exudative AMD patients are showing early degenerative changes occurring at the level of the retina or along the visual pathways.

Although amplitude attenuation and latency delays have been demonstrated in macular disease [9, 10, 12, 13, 15, 16, 29], debate persists regarding the distinguishing features in the VEP response between retinal damage and optic neuropathy [7, 14, 32]. The mfVEP changes observed in our study are in agreement with the findings of Shimada et al. [15]. They recorded significant amplitude changes with conventional high-contrast VEP stimuli in eyes with macular disease but no significant delay relative to the unaffected eye. However, only three eyes from their series presented with AMD. Recently, Walter et al. [29] reported reduced pattern-reversal VEP amplitudes and prolonged latencies in 43 AMD eyes, although nine subjects had unexpectedly greater attenuation from the foveal field (3°) than the macular field (13°). The results of our study were different, in that amplitude responses were more significantly affected than delay in both early and advanced AMD. The prolongation of the time-to-peak responses observed in our group was significantly less than that observed in macular disease [15, 16, 29] and optic neuritis [20, 32]. This discrepancy in results may be due to differences in stimulus conditions and possibly aspects of the gfRMS waveform. To confirm that pooling electrode responses (gfRMS) was an improvement on standard practice, we examined the raw waveforms from a single channel (POz) and found that on average the effect of AMD on POz amplitudes diminished by up to 46 %. Recently published results on dichoptic mfVEP responses in multiple sclerosis [5] showed significantly longer delays than those found in our series of AMD eyes; however, mean amplitude attenuation was similar, confirming previous reports [14, 32]. Results of mfVEP recordings by Chen et al. showed that latencies observed in retinal disease correspond closely to those found in optic neuritis/multiple sclerosis. The reason for the prolonged latency in multiple sclerosis relative to maculopathy with our technique is uncertain. It may

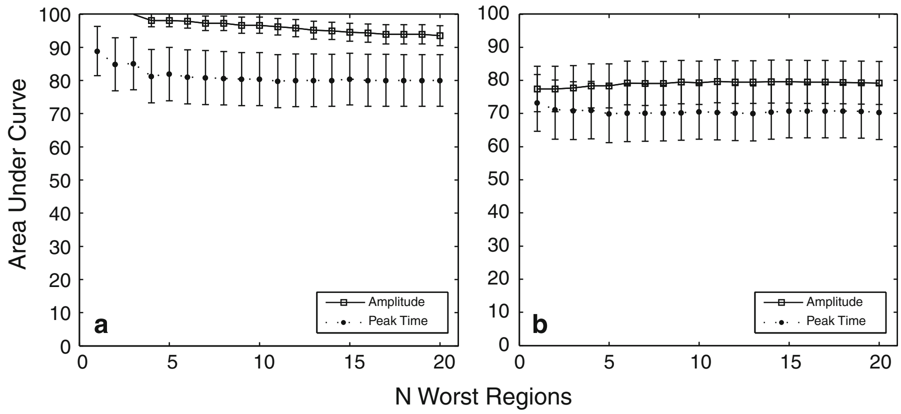

Fig. 8 ROC (AUC) ± SE plots for the mean of *n*-worst deviations for **a** exudative AMD and **b** non-exudative AMD subjects from the normative data. Two parameters of the mean response from the occipital channels ("Methods") which are considered are amplitude and peak time. **a** represents deviations between regional responses of the left and right eyes compared to normal eyes. That is, diseased eyes showed much greater asymmetry between eyes than that of normal subjects. **b** considers deviations of each region from the same eye

be due to the difference in recording and analysis method used and the variation in pathophysiology of the macular disease investigated. Our results are in agreement with a previous clinical study utilizing multifocal pupillographic objective perimetry in the same group of AMD subjects measured on the same day as their mfVEP tests [24]. In this study, significantly quicker time-to-peak responses were measured in two of four regions in the central 6° of the visual field (Fig. 3b) equivalent to approximately the central two rings of our mfVEP stimulus (subtending ± 3.7° of the visual field). Mean retinal thickness values measured by OCT tended to show more thickening in the central 1 mm diameter (central ± 3.3° of fixation) in exudative AMD eyes (14 of 19 eyes) corresponding to the regions with quicker time-to-peak responses in both mfVEP and mfPOP [24]. A possible mechanism for the slight decrease in delay in VEP responses in central regions of the patients is that as the rods die, there is greater oxygen available to the cones as has been shown in P23H rats [33, 34]. Even in bright light rods consume considerable oxygen [35], and in the retinal regions stimulated by our inner three rings, there are normally about 4–5 times more rods than cones [36]. Cone-isolating ERGs from P23H rats diminish in size out 550 post-natal days, but do not seem to show any change in delay [34]. Thus, the rat cones seem to be sustained by the extra oxygen if not accelerated.

The ROC analysis shown in Fig. 8 indicates that amplitude deviations produced higher AUCs in eyes with more severe damage. Interocular comparisons achieved higher diagnostic power than within-eye deviations, suggesting that bilateral presentations may potentially reduce AUC values. In advanced macular disease, several regions would be expected to give 100 % sensitivity and specificity (Fig. 8a); however, even considering the *worst* 20 regions in the field (akin to the mean deviation), AUC values were approximately constant at 93 %. The AUC of 79.7 % obtained for non-exudative AMD suggests that it preforms slightly better than contrast sensitivity (69 %) and SAP (60 %) in early AMD [37]. The observed discrepancy between amplitude and delay deviations for early- and late-stage AMD suggests that anatomical disruptions to the outer retina in mild presentations may alter synaptic transmission affecting the temporal component of the response initially. Similar results in mfERG studies of early AMD [38] and diabetic [39] eyes have been reported.

There were several limitations in this study. Patients with exudative AMD develop an eccentric fixation position known as preferred retinal locus [40, 41] (PRL) leading to poor fixation stability [42]. Our results may not accurately reflect responses from test regions in the exudative eye if a PRL is active; however, recent evidence suggests that under dichoptic conditions ocular motor control is driven by the better acuity eye and fixation stability improves in the worse acuity eye [43]. A limitation of the mfVEP technique is the dynamic range required to estimate depths of scotomata. Accordingly, we applied temporally sparse stimuli to produce higher signal-to-noise ratios [19] than conventional contrast-reversing mfVEP in order to maximize the dynamic range of the signal and improve diagnosticity. In addition, the sample size was relatively small, and selection criteria restricted the inclusion of subjects with similar disease presentations between eyes. Exudative AMD eyes were all concurrently treated with ranibizumab intravitreal injections; consequently, responses may have been influenced by pharmaceutical agents and not representative of the true disease state.

In conclusion, this study is the first demonstration of significant reduction in mean mfVEP amplitudes and response delays in the macular field in both exudative and non-exudative AMD eyes. Peripheral retinal areas were less affected (8.4°–23.0°); however, there was a trend towards further decline beyond these eccentricities. The diagnostic performance and reduced testing duration of dichoptic mfVEPs suggest that this technique may have clinical utility in assessing early AMD and the long-term monitoring of progression. Future investigations with larger study samples are required to examine reproducibility and spatial relationships between mfVEP abnormalities and local retinal lesions.

Acknowledgments The authors thank Australian Research Council (ARC) through the ARC Centre of Excellence in Vision Science (CE0561903), AusIndustry and Seeing Machines Ltd, Canberra.

References

1. Regan D, Heron JR (1969) Clinical investigation of lesions of the visual pathway: a new objective technique. J Neurol Neurosurg Psychiatry 32(5):479–483
2. Milner BA, Regan D, Heron JR (1974) Differential diagnosis of multiple sclerosis by visual evoked potential recording. Brain 97(4):755–772
3. Cappin JM, Nissim S (1975) Visual evoked responses in the assessment of field defects in glaucoma. Arch Ophthalmol 93(1):9–18
4. Baseler HA, Sutter EE, Klein SA, Carney T (1994) The topography of visual evoked response properties across the visual field. Electroencephalogr Clin Neurophysiol 90(1):65–81
5. Ruseckaite R, Maddess T, Danta G, Lueck CJ, James AC (2005) Sparse multifocal stimuli for the detection of multiple sclerosis. Ann Neurol 57(6):904–913
6. Hood DC, Zhang X, Greenstein VC, Kangovi S, Odel JG, Liebmann JM, Ritch R (2000) An interocular comparison of the multifocal VEP: a possible technique for detecting local damage to the optic nerve. Invest Ophthalmol Vis Sci 41(6):1580–1587
7. Chen JY, Hood DC, Odel JG, Behrens MM (2006) The effects of retinal abnormalities on the multifocal visual evoked potential. Invest Ophthalmol Vis Sci 47(10):4378–4385
8. Wolff BE, Bearse MA Jr, Schneck ME, Barez S, Adams AJ (2010) Multifocal VEP (mfVEP) reveals abnormal neuronal delays in diabetes. Doc Ophthalmol 121(3):189–196
9. Lennerstrand G (1982) Delayed visual evoked cortical potentials in retinal disease. Acta Ophthalmol (Copenh) 60(4):497–504
10. Marcus M, Merin S, Wolf M, Feinsod M (1983) Electrophysiologic tests in assessment of senile macular degeneration. Ann Ophthalmol 15(3):235–238
11. Folk JC, Thompson HS, Han DP, Brown CK (1984) Visual function abnormalities in central serous retinopathy. Arch Ophthalmol 102(9):1299–1302
12. Bass SJ, Sherman J, Bodis-Wollner I, Nath S (1985) Visual evoked potentials in macular disease. Invest Ophthalmol Vis Sci 26(8):1071–1074
13. Sherman J, Bass SJ, Noble KG, Nath S, Sutija V (1986) Visual evoked potential (VEP) delays in central serous choroidopathy. Invest Ophthalmol Vis Sci 27(2):214–221
14. Johnson LN, Yee RD, Hepler RS, Martin DA (1987) Alteration of the visual evoked potential by macular holes: comparison with optic neuritis. Graefes Arch Clin Exp Ophthalmol 225(2):123–128
15. Shimada Y, Adachi-Usami E, Murayama K (1997) How are macular changes reflected in pattern visually evoked cortical potentials? Acta Ophthalmol Scand 75(3):277–280
16. Negishi C, Takasoh M, Fujimoto N, Tsuyama Y, Adachi-Usami E (2001) Visual evoked potentials in relation to visual acuity in macular disease. Acta Ophthalmol Scand 79(3):271–276
17. Rosli Y, Xin-Lin G, James A, Maddess T (2008) Neural signal processing of mfVEP responses from AMD patients. In: Information technology. International symposium on, pp 1–6
18. James AC (2003) The pattern-pulse multifocal visual evoked potential. Invest Ophthalmol Vis Sci 44(2):879–890
19. James AC, Ruseckaite R, Maddess T (2005) Effect of temporal sparseness and dichoptic presentation on multifocal visual evoked potentials. Vis Neurosci 22(1):45–54
20. Maddess T, James AC, Bowman EA (2005) Contrast response of temporally sparse dichoptic multifocal visual evoked potentials. Vis Neurosci 22(2):153–162
21. James AC, Maddess T, Goh XL, Winkles N (2005) Spatially sparse pattern-pulse stimulation enhances multifocal visual evoked potential analysis. Invest Ophthalmol Vis Sci 46(5):3602
22. Bland JM, Altman DG (1986) Statistical methods for assessing agreement between two methods of clinical measurement. Lancet 1(8476):307–310
23. Bell A, James AC, Kolic M, Essex RW, Maddess T (2010) Dichoptic multifocal pupillography reveals afferent visual field defects in early type 2 diabetes. Invest Ophthalmol Vis Sci 51(1):602–608
24. Sabeti F, Maddess T, Essex RW, James AC (2011) Multifocal pupillographic assessment of age-related macular degeneration. Optom Vis Sci 88(12):1477–1485
25. Stensaas SS, Eddington DK, Dobelle WH (1974) The topography and variability of the primary visual cortex in man. J Neurosurg 40(6):747–755

26. Rademacher J, Caviness VS Jr, Steinmetz H, Galaburda AM (1993) Topographical variation of the human primary cortices: implications for neuroimaging, brain mapping, and neurobiology. Cereb Cortex 3(4):313–329
27. Curcio CA, Medeiros NE, Millican CL (1996) Photoreceptor loss in age-related macular degeneration. Invest Ophthalmol Vis Sci 37(7):1236–1249
28. Sokol S (1972) An electrodiagnostic index of macular degeneration. Use of a checkerboard pattern stimulus. Arch Ophthalmol 88(6):619–624
29. Walter P, Konigsfeld P, Soudavar F, Brunner R (2000) Unusual visual evoked potentials in patients with age-related macular degeneration. Ophthalmologica 214(5):312–319
30. Graham SL, Klistorner AI, Grigg JR, Billson FA (2000) Objective VEP perimetry in glaucoma: asymmetry analysis to identify early deficits. J Glaucoma 9(1):10–19
31. Gin TJ, Luu CD, Guymer RH (2011) Central retinal function as measured by the multifocal electroretinogram and flicker perimetry in early age-related macular degeneration. Invest Ophthalmol Vis Sci 52(12):9267–9274
32. Han DP, Thompson HS, Folk JC (1985) Differentiation between recently resolved optic neuritis and central serous retinopathy. Use of tests of visual function. Arch Ophthalmol 103(3):394–396
33. Yu DY, Cringle S, Valter K, Walsh N, Lee D, Stone J (2004) Photoreceptor death, trophic factor expression, retinal oxygen status, and photoreceptor function in the P23H rat. Invest Ophthalmol Vis Sci 45(6):2013–2019
34. Chrysostomou V, Stone J, Valter K (2009) Life history of cones in the rhodopsin-mutant P23H-3 rat: evidence of long-term survival. Invest Ophthalmol Vis Sci 50(5): 2407–2416
35. Okawa H, Sampath AP, Laughlin SB, Fain GL (2008) ATP consumption by mammalian rod photoreceptors in darkness and in light. Curr Biol 18(24):1917–1921
36. Curcio CA, Sloan KR, Kalina RE, Hendrickson AE (1990) Human photoreceptor topography. J Comp Neurol 292(4): 497–523
37. Ivers RQ, Optom B, Macaskill P, Cumming RG, Mitchell P (2001) Sensitivity and specificity of tests to detect eye disease in an older population. Ophthalmology 108(5):968–975
38. Gerth C, Hauser D, Delahunt PB, Morse LS, Werner JS (2003) Assessment of multifocal electroretinogram abnormalities and their relation to morphologic characteristics in patients with large drusen. Arch Ophthalmol 121(10):1404–1414
39. Fortune B, Schneck ME, Adams AJ (1999) Multifocal electroretinogram delays reveal local retinal dysfunction in early diabetic retinopathy. Invest Ophthalmol Vis Sci 40(11): 2638–2651
40. White JM, Bedell HE (1990) The oculomotor reference in humans with bilateral macular disease. Invest Ophthalmol Vis Sci 31(6):1149–1161
41. Schuchard RA (2005) Preferred retinal loci and macular scotoma characteristics in patients with age-related macular degeneration. Can J Ophthalmol 40(3):303–312
42. Timberlake GT, Mainster MA, Peli E, Augliere RA, Essock EA, Arend LE (1986) Reading with a macular scotoma. I. Retinal location of scotoma and fixation area. Invest Ophthalmol Vis Sci 27(7):1137–1147
43. Tarita-Nistor L, Brent MH, Steinbach MJ, Gonzalez EG (2011) Fixation stability during binocular viewing in patients with age-related macular degeneration. Invest Ophthalmol Vis Sci 52(3):1887–1893